IEEE Access
Multidisciplinary | Rapid Review | Open Access Journal

Received December 13, 2019, accepted December 22, 2019, date of publication December 25, 2019,
date of current version January 7, 2020.

Digital Object Identifier 10.1109/ACCESS.2019.2962324

Integrated Multichannel Electrochemical–Quartz Crystal Microbalance Sensors for Liquid Sensing

**AHMAD ANWAR ZAINUDDIN[1], (Student Member, IEEE),
ANIS NURASHIKIN NORDIN[1], (Senior Member, IEEE),
AHMAD FAIRUZABADI MOHD MANSOR[1], (Student Member, IEEE),
ROSMINAZUIN AB RAHIM[1], (Member, IEEE), AND WING CHEUNG MAK[2]**

[1]Department of Electrical and Computer Engineering, Kulliyyah of Engineering, International Islamic University Malaysia, Kuala Lumpur 50728, Malaysia
[2]Biosensors and Bioelectronics Centre, Department of Physics, Chemistry and Biology (IFM), Linkoping University, 58183 Linkoping, Sweden

Corresponding authors: Anis Nurashikin Nordin (anisnn@iium.edu.my) and Wing Cheung Mak (wing.cheung.mak@liu.se)

This work was supported in part by the Swedish Research Council under Grant VR-2014-43058, and in part by the Malaysian Ministry of Higher Education under Grant FRGS15-217-0458.

ABSTRACT This paper highlights the design, simulation and fabrication of an array of twelve integrated electrochemical – quartz crystal microbalance (IEQCM) sensors on a single substrate for liquid sensing. Integration of both measurement techniques is made possible by combining the three electrode electrochemical device with the top and bottom electrodes for the microbalance. Important design parameters such as the working electrode radius and gap spacing, were studied using both theoretical calculations and COMSOL Multiphysics® finite element simulations. The sensor's working electrode radius affects the magnitude of the frequency response while the gap affects the capacitance and current density which are important for electrochemical measurements. It was found that the best values for the working electrode radius was 2 mm and gap spacing was 0.5 mm. The sensors were fabricated using microfabrication techniques for the gold electrode and screen printing techniques for the reference electrode. Water contact angle, atomic force microscopy, and scanning electron microscope were utilized to study the surface roughness of the IEQCM sensor. IEQCM has a low contact angle of 53.0 ± 1° and low surface roughness of 1.92nm. For liquid sensing, an array of circular chambers were fabricated using polydimethylsiloxane (PDMS) and placed on top of the quartz substrate for liquid testing. Electrochemical measurements and cyclic voltammetry were performed using the sensor in ferri-ferrocyanide and phosphate buffered saline solution to study the function of scan rates on the peak current with respect to the potential difference. For mass sensing measurements, liquid water droplets of 1uL – 10 uL were placed onto the sensing surface and the change in resonance frequencies of the sensors were measured. These resonance frequency changes can be converted in mass change/area in accordance to the advanced Sauerbrey equation. The multichannel IEQCM sensor shows good potential as a parallel sensor for both biosensing and environmental applications.

INDEX TERMS Quartz crystal microbalance (QCM), electrochemical impedance spectroscopy (EIS), sensor arrays, microelectromechanical devices, mass spectroscopy, and acoustic devices.

I. INTRODUCTION

Quartz crystal microbalances (QCM) are thickness-shear mode bulk acoustic wave transducers that can be used for physical, chemical and biological sensing applications [1]–[5]. These acoustic wave sensors can detect interfacial mass changes on the crystal's surface by monitoring frequency response changes of the QCM's oscillation frequency [6]. Resonant frequencies of the QCM are dependent on the crystal's thickness, with thinner crystals producing

The associate editor coordinating the review of this manuscript and approving it for publication was Norbert Herencsar.

higher resonant frequencies. When acting as a sensor, the resonant frequency of the QCM is influenced by external physical loading, either gravimetric or viscoelastic loading. The main advantages of QCM sensors are that they do not require calibration, have high sensitivities, stability, provide real-time measurements and are low cost. When used as biosensors, it has an added advantage of being a label-free sensor. The typical configuration of QCM is a single element sensor, but multichannel QCM array have also been proposed [7], [8]. QCM arrays can help to minimize effects of variations in environmental parameters such as temperature. This can be more practically achieved when two or more QCMs are fabricated on a single quartz substrate which is also known as monolithic multichannel QCMs or MQCMs [9]. The design of MQCMs have to take into account acoustic interference problems in which mass or stress loading on one QCM will induce spurious frequency shift on the other [10]. Despite these drawbacks, MQCMs remain attractive as they lead to reduction in cost, diagnostic time and sample volume [11].

Apart from QCM sensors, electrochemical sensors have also been widely used to capture biological recognition targets and events that can directly translate results into electrical signals. Electrochemical sensors can be used to monitor signal responses such as current or impedance resulting from oxidation-reduction of redox species. These signal responses can be measured via electrochemical detection techniques such as cyclic voltammetry (CV) and electrochemical impedance spectroscopy (EIS).

In recent years, these two measuring techniques (mass-sensing and electrochemical detection) have been combined to form a single electrochemical quartz crystal microbalance (EQCM) sensor. The EQCM sensor can be used to obtain precise, quantitative information in biological and chemical systems [12], [13]. In general, EQCM sensors comprise of quartz crystal microbalance sensor (QCM) integrated with both counter and reference electrodes of the electrochemical sensor in a single measurement platform. The main advantage of these integrated sensors is that it can measure both resonance frequency changes and electrochemical reactions in parallel. In this paper, we have designed an array of twelve integrated electrochemical and quartz crystal microbalance sensors (IEQCM) on a single quartz substrate. Each sensor is a three-electrode system which can perform *in-situ* measurements of the electrode's surface changes based on piezoelectric and electrochemical transductions. This multichannel device offers advantages of being real-time, capable of conducting both electrochemical and frequency response measurements, portable and requiring low sample volumes.

The novelty of this improved work with respect to our previous ones [14]–[17] lies in the experimental verification of both the QCM and integrated electrochemical sensor. Our previous work concentrated on the modeling and resonance measurements of the QCM and no experimental measurements on the integrated electrochemical sensor had been done. In this work, the functionality of the integrated EQCM sensors have been tested with water for mass sensing and with ferri-ferrocyanide and Phosphate B uffered Saline (PBS) for electrochemical sensing.

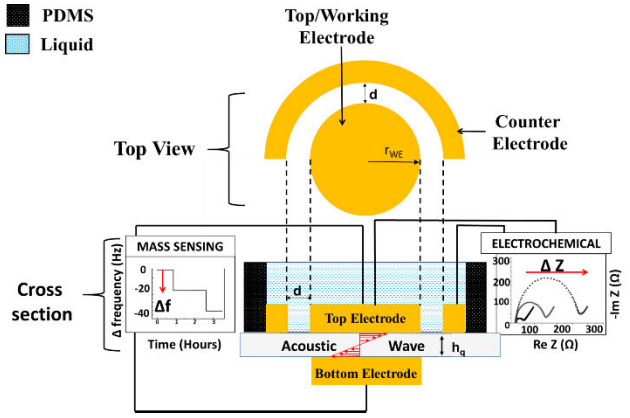

FIGURE 1. Integrated quartz crystal microbalance and electrochemical sensor: top view, cross-section and conceptual diagram. The electrochemical electrodes: counter and working electrode measures change in impedance. The top and bottom electrodes of the QCM sensor can detect changes in mass by measurements of changes in the resonant frequency.

The organization of this report is as follows: The first section introduces the basic principles of sensing for QCM and electrochemical sensors. The current issues of QCM and electrochemical sensor are also highlighted in this section. Section II introduces our proposed design of a novel integrated mass and an electrochemical sensor. Section III explains the finite element modelling of the sensor performed using COMSOL. The fabrication process was described in Section IV. Section V and VI presented measurement results and discussion. Section VII concludes this work.

II. SENSING PRINCIPLE AND DESIGN THEORY

Fig. 1 shows the conceptual diagram of the integrated QCM with electrochemical sensing capabilities. The electrochemical sensor comprises of two electrodes, counter and working electrode. The circular working electrode also acts as the top electrode of the QCM. The QCM detects mass by the shift in resonance frequencies. The electrochemical measurements are done via the top two electrodes. The variables r_{WE}, w_{CE}, d and h_q indicate the radius of working electrode, width of counter electrode, gap between electrodes and quartz thickness respectively.

A. QUARTZ CRYSTAL MICROBALANCE

To increase the sensitivity of QCM, a very thin quartz crystal is required as it will produce higher resonance frequency [18]. **Fig. 2** shows the effect of varying quartz thickness, h_q on resonance frequency, f_0. It can be seen that when the quartz's thickness is increased the resonance frequency is reduced.

For this work, large-diameter (76.2 mm) quartz wafers were used to fit twelve multichannel biosensors on a single substrate. For easy handling, thickness of 500 μm was chosen for the quartz wafer. All the sensors operate at the resonance

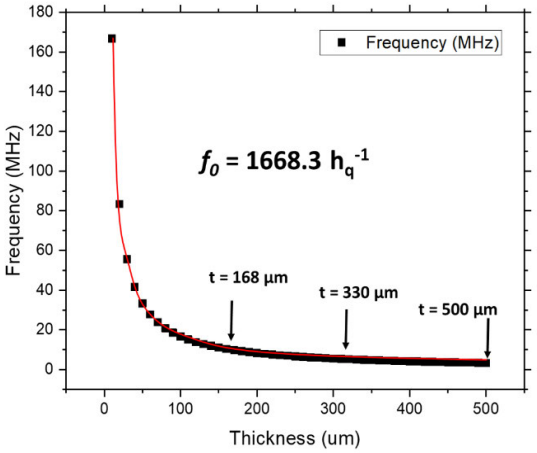

FIGURE 2. The effect of varying quartz thickness, h_q on resonance frequency, f_0 derived from Eq. (1). The typical quartz thicknesses of 168 μm, 330 μm and 500 μm which correspond to 10 MHz, 5 MHz and 3 MHz, respectively.

frequency of 3MHz with minimal interference. Other than the diameter and thickness of quartz wafer, the radius of the working electrode also influences mass sensitivity. Smaller electrode radius will reduce mass sensitivity due to larger resistance [19]. The advanced Sauerbrey equation is used to describe the relationship between the resonant frequency shift and mass change in liquids, taking into account the fact that the acoustic waves are damped by the liquid and cause energy dissipation [20]. This affects the density, viscosity and acoustic impedance. Change of frequency and change of mass is expressed in Eq. (1) [21], [22] as:

$$\Delta m = \frac{\frac{\Delta f}{f_0}\left(\rho_q h_q\right)}{\left[1-\left(\frac{\rho_l}{\rho_f} Re \frac{\mu_l}{\mu_f}\right)\right]} \tag{1}$$

where Δf is the resonant frequency shift (Hz), Δm is the mass change per area (μg/cm^2). ρ, η and μ is the density, viscosity and shear modulus with indices l, f, and q indicating the liquid, film (electrode), and quartz respectively. All the material properties used in this work have been detailed in [17].

B. ELECTROCHEMICAL SENSOR

The electrode design needs to be optimized both for mass and electrochemical sensing. The most crucial parameter of electrochemical sensor is the gap between electrodes, d. The electrochemical sensor detects electric signal changes such as current, impedance or capacitance in the electrode surface due to redox reaction. Typically, this sensor uses the three-electrode system which consists of working (*WE*), counter (*CE*) and a reference electrode (*RE*). Optimization of the current density and total capacitance can be achieved by varying d. Higher current density and total capacitance are required to allow faster rate of reduction and oxidation [23].

The Butler-Volmer equation relates current density with total capacitance over the electrode surface area [24]. The current density is also directly proportional to the applied voltage ($V_{applied}$) and I_{sensor}, considering that both cathodic and anodic reaction occurs on the same electrode. Based on the Butler-Volmer equation, constant phase element (CPE) is directly proportional to current density. This means an increase in CPE increases current density and also the sensor's sensitivity. On the other hand, the active geometric area is inversely proportional to current density, therefore decreasing geometric area increases current density. Based on this theory, the current density is directly proportional to the total capacitance (C_{total}) of the system, based on Eq. (2) [24]:

$$i_0 = \frac{I_{sensor} C_{total}\, j\omega V_{applied}}{A_{geo}\left(e^{\left[\frac{(1-\alpha)nF}{RT}(E-E_{eq})\right]} - e^{\left[\frac{\alpha nF}{RT}(E-E_{eq})\right]}\right)} \tag{2}$$

where;

A_{geo} = electrode active geometry surface area, m^2
I_{sensor} = total sensing current, A
C_{total} = total capacitance = CPE, F
i_o = current density, A/m^2
E = electrode potential, V
E_{eq} = equilibrium potential, V
T = absolute temperature, K
n = number of electrons involved in the electrode reaction
F = Faraday's constant
R = universal gas constant
α = symmetry factor = 0.5
$V_{applied}$ = applied potential, V

Reducing d will increase the total capacitance or *CPE* as well as maximize the current density of the sensor [25].

III. FINITE ELEMENT SIMULATION MODEL

Both mechanical resonance frequency and electrochemical operation in the IEQCM were simulated using COMSOL Multiphysics® software for more accurate finite element simulations. In the first simulation, resonance frequency analysis was performed on a single QCM to find its resonance frequency and overtones. The effect of varying radius to the resonance frequency was also simulated. Next, the current density analysis was done to determine the optimum design for the electrochemical sensor. The COMSOL Multiphysics®QCM model consists of an AT-cut quartz crystal with two circular top and bottom electrodes. The thickness of AT-cut quartz crystal and the gold electrode was set to 500 μm and 200 nm, respectively. An AC signal of 0.5V was applied on the top working electrode, and the other electrode was grounded.The total mechanical displacement of the crystal with different radii of the top and bottom electrodes were studied. **Fig. 3(a)** shows the effect of varying the radius of the electrodes from 100 μm to 2000 μm on mechanical displacement. From the results, it was seen that increasing the radius will result in an increase in total displacement at resonance. Large electrode radius allows higher acoustic energy trapping and lower energy losses to the surroundings. This results in higher quality factors or Q as shown in **Fig. 3(a)** where the largest radius, r_{we} = 2000 um produced the highest Q = 332.

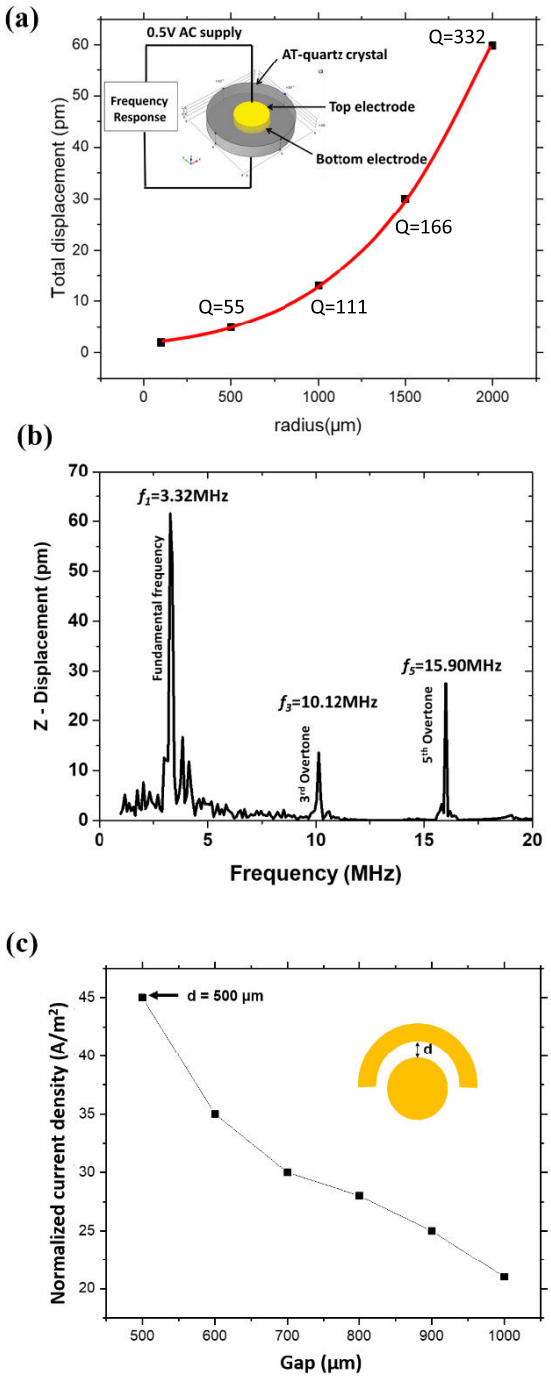

FIGURE 3. **(a) Effect of varying radius of the working electrode on the total mechanical displacement of the quartz crystal. The size of the working electrode was varied from 100 μm to 2000 μm. Inset shows the boundary condition setup using piezoelectric MEMS module for a single QCM sensor in a single disk. (b) Resonance frequency simulation of r_{we} = 2000μm. The 1st, 2nd and 3rd overtone were found at f_0 = 3.32MHz, f_1 = 10.12MHz and f_3 = 15.90MHz, respectively. (c) Optimization of gap, d between counter and working electrode. Gap was varied between 500 −1000 um. Normalized current density is inversely proportional to gap.**

The quartz crystal also produces several harmonics or overtones as shown in **Fig. 3(b).** For this analysis, the largest radius or r_{we} = 2000 um was chosen and the overtones and their z-displacements were plotted. The highest displacement is shown at 1st overtone, which corresponds to 3.32 MHz. The other two overtones were at 10.12 MHz and 15.90 MHz have significantly lower Z-displacement magnitudes.

In the next simulation, the gap, d between the working and the counter electrodes is studied. **Fig. 3(c)** shows the simulation of normalized current density with d from 500 μm to 1000 μm. Smaller gaps produced increased current densities, with the smallest gap of 500 μm producing current density of 45 A/m^2. The gap also affects the capacitance values between the working and counter electrode with the highest total capacitance is simulated to be 0.36 pF at d = 500 μm. For this work, d = 500 μm was chosen to maximize current density.

IV. EXPERIMENTAL WORK

A. FABRICATION PROCESS

As the sensor is aimed for biological applications, gold was chosen for the working and counter electrodes. Gold allows formation of self-assembled monolayers via covalent bonding between gold and thiols [16], [26]. The fabrication process of the IEQCM on a quartz substrate is described in **Fig. 4(a)**. Prior to e-beam process, all quartz substrates and shadow masks were cleaned in TL1 solution method (1:1:5 proportions of 25% NH_3, 30% H_2O_2, and Milli-Q water for 10 min at 85°C), washed with Milli-Q (18.2 MΩ) water several times and dried in N_2 stream. Titanium and gold evaporation beam (e-beam) processes were done on the front side and back side (sandwich layer) of quartz surface using a shadow mask. A 20 nm titanium adhesion layer was evaporated at a rate of 0.3 – 0.5 Å s^{-1} on the quartz wafer. Next, 200 nm thick gold layer was evaporated at 10 Å s^{-1} under vacuum. The reference electrode was realized via screen-printing technique. This technique prints the silver/silver chloride paste (C61003P7, Gwent Electronics Materials Ltd, UK) through a screen mesh to form Ag/AgCl films. This technique prints the silver/silver chloride paste (C61003P7, Gwent Electronics Materials Ltd, UK) through a screen mesh to form Ag/AgCl films. Circular chambers with diameter of 5.5 mm and volume of 40μl were made using polydimethylsiloxane (PDMS) and placed on top of the quartz substrate to allow liquid testing. As a final step, the IEQCM is placed on a FR4 board with connector pins as shown in **Fig. 4(b).**

B. SURFACE ROUGHNESS AND WETTABILITY CHARACTERIZATION

Wettability of a sensor's surface can be investigated by measuring contact angle of water droplets on the gold surface. Contact angle measurements are usually done to measure hydrophobicity or hydrophilicity of a material. Wettability also indicates the quality of the modified surface, where lower contact angles promote molecule immobilization [27]. In this work, the hydrophobicity of the fabricated gold electrodes were measured using a digital camera (CAM 200 Optical Contact Angle meter. A drop of 5 μL deionized water was placed on the working electrode's surface (**Fig. 5(a)**) and

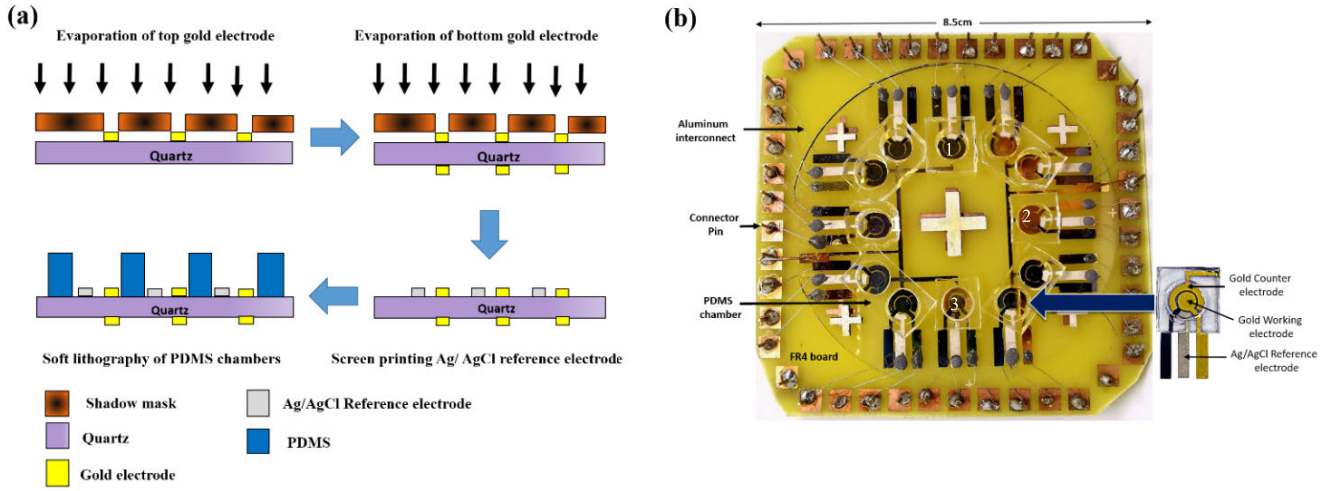

FIGURE 4. (a) Fabrication process flow of the IEQCM sensor: Clockwise from left: Shadow mask was used to pattern the working and counter electrodes onto the top quartz substrate via evaporation process. This process was repeated using to pattern the bottom electrodes onto the quartz substrate. Next, screen printing process was used to realize the Ag/AgCl reference electrode. Finally, soft lithography process was used to create PDMS chambers for each sensor (b) Photograph of IEQCM sensor-on-board with its interconnects. Sensors that were used in the experiments are labelled as 1, 2 and 3.

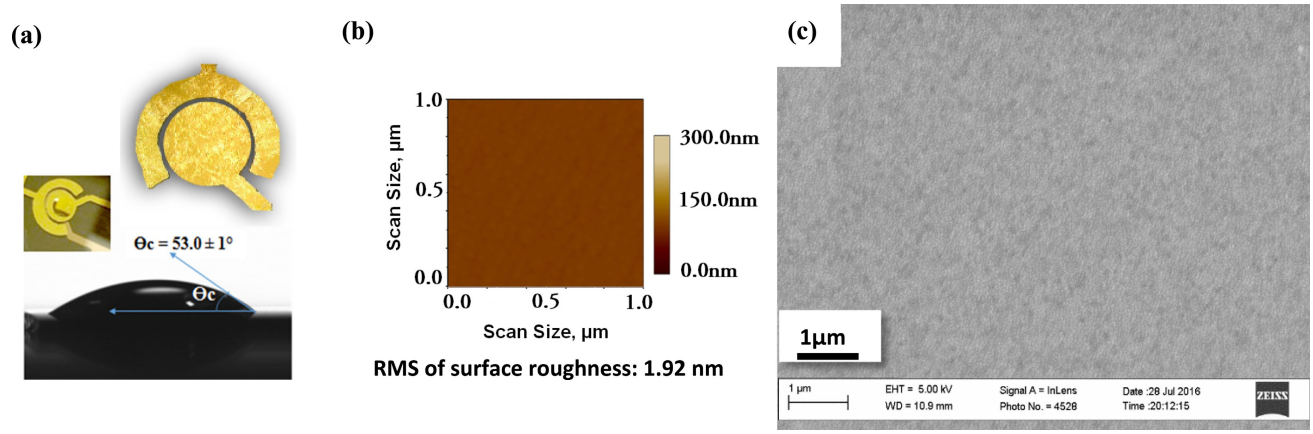

FIGURE 5. Surface roughness characterization. (a) Optical images of IEQCM and Water contact angle measurement for wettability test. (b) 2D AFM surface roughness profile of the gold electrode. (c) SEM image indicating the surface morphology of the electrode.

the water contact angle was measured. The average contact angle value was calculated from triplicate measurements. The volume and the size of the drops were kept constant. From the results, the measured contact angle of IEQCM sensor was 53.0 ± 1°. Measured values of less than 90° indicate that the surface is hydrophilic [28]. As a comparison, the contact angle for a bare screen-printed gold electrode was also measured and found to be 109.412 ±0.3°.

Next, surface roughness of the evaporated gold electrodes was measured using an atomic force microscope (AFM), NanoScope IVa Dimension 3100 SPM from Veeco Instruments, Inc.,USA. The topography of the gold electrode was measured using tapping mode over a 1 $\times$1 μm^2 area was shown in **Fig. 5(b)**. Root mean square of the surface roughness for the gold electrodes was measured to be 1.92 nm. This surface roughness of the evaporated gold electrode is significantly lower than those of commercial screen printed gold electrodes which have surface roughness of 33.23 nm.

Finally, the surface morphology of IEQCM was examined using a scanning electron microscope (SEM) LEO 1550 Gemini, Zeiss, Germany, shows the gold coating has a relatively homogenous surface morphology **Fig 5(c)**. The uniform and smooth gold electrodes was achieved using electron-beam vacuum evaporation. Compared to screen printing, evaporation method yields thin films with higher film density and increased adhesion to the substrate [29]. The evaporation process also produces better quality of gold electrodes as it creates a relatively homogenous gold layer for bioconjugation and hydrophilicity towards biomolecules that facilitates the attachment of biorecognition molecules on the electrode [30].

C. QCM RESONANT FREQUENCY MEASUREMENTS

Resonance frequency measurements of the IEQCM were measured using an E5061B Agilent Vector Network Analyzer. The resonance frequency and its harmonics for an individual IEQCM sensor were measured to be 3.28 MHz,

9.84 MHz and 15.87 MHz for the 1st, 2nd and 3rd overtones respectively. Based on the theoretical calculations using Eq. (1), the resonance frequency was calculated to be 3.34MHz, 10.00MHz and 16.70MHz for the 1st, 2nd and 3rd overtones, respectively. Therefore, these measurement results showed a good agreement with theory and simulation results since they exhibited small tolerance of 1.7%, 1.6% and 4.9% which corresponded to the 1st, 2nd and 3rd overtones. For our work, the frequency measurements of three different QCMs on a single quartz wafer were made. The minimum center-to-center distance between adjacent sensors is 8.1 mm. The resonance frequencies of Sensor 1, 2 and 3 were measured to be 3.2873 MHz, 3.2835 MHz and 3.2643 MHz respectively. Distinct resonant frequencies of each sensor indicate that the minimal spacing of 8.1 mm is sufficient to reduce acoustic interference.

To evaluate and verify the effect of liquid loading on the QCM, liquid droplets of water were placed onto the sensors and resonance frequency changes were measured. One uL drops were loaded at the center of each sensor to a total of 10 uL. Incremental addition of droplets were done over time to avoid placing the droplets on different locations on the electrode. The QCMs have spatial sensitivities and mass sensitivities are not uniform throughout the sensor's surface [31]. Evaporation of water droplets was assumed negligible since the experiments were conducted conservatively in a short time (3-5 seconds) in order to obtain stable measurements for each data point. Three different sensors were used and the measured frequency shifts versus increasing volume were plotted as shown in **Fig. 6(a)**. As comparison, the theoretical frequency shifts were calculated using Equation (1) and also plotted in the same graph. The frequency shift versus volume is relatively linear in the measured range. Frequency shifts can be translated into mass changes using Equation (1) and are plotted for both experimental and theoretical values as shown in **Fig. 6(b)**. Although both experimental graphs are linear, there exists mass underestimations when compared to the theoretical calculations based on Sauerbrey equation. This 'missing mass' phenomenon has been reported by other researchers when when QCMs are loaded with heavy, non-rigid masses [32]. This may be due to energy dissipations caused by build-up of bulky viscoelastic mass resulting in non-uniform vibrations in the QCM [32]. QCM sensors are also spatial sensitive where the mass sensitivity versus position function for a QCM sensor is approximately Gaussian where the mass-sensitivity maximum is at the center of the electrode and tapers off towards the edge of the electrode [31], [32]. For this experiment, the water droplets were pipetted manually and due to the miniature size of the sensor, it was difficult to control the exact location of the droplets. It is hypothesized that the slight shift in location of the droplets produce the errors.

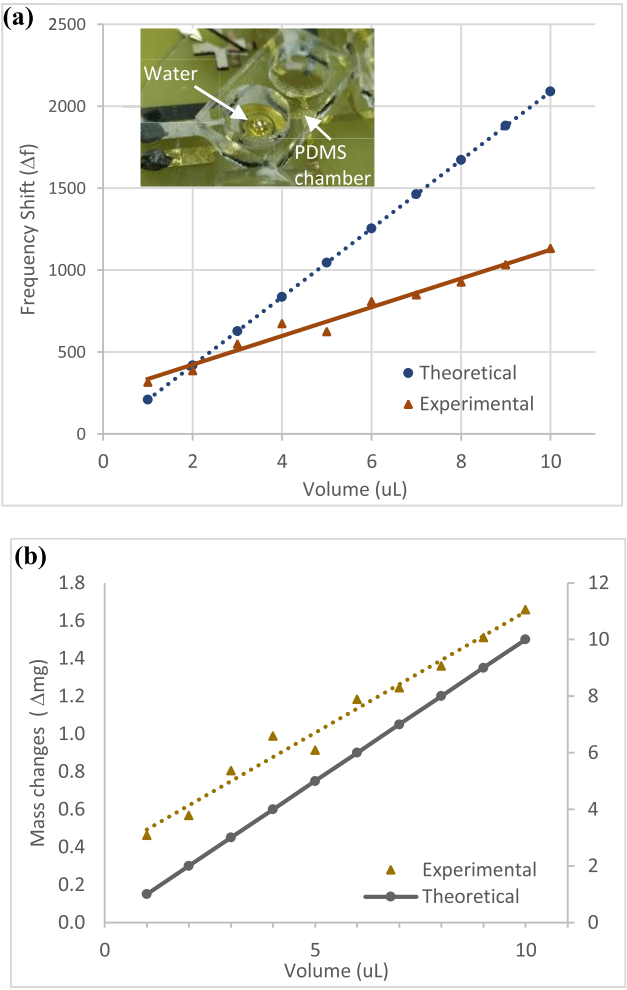

FIGURE 6. **(a) Measurement of resonant frequency changes of the IEQCM sensors at different volumes of water. Three different sensors were used in the experiment and measurements were taken in triplicates. The average measurements are plotted in the graph. Theoretical calculations of the resonant frequency shift based on Sauerbrey equation are also plotted. Inset: Liquid water droplet placed at the center of the QCM. (b) Mass change measurement and theoretical values.**

D. ELECTROCHEMICAL SENSING

To verify the functionality of the electrochemical sensor within the IEQCM, electrochemical measurements such as cyclic voltammetry (CV) and electrochemical impedance spectroscopy (EIS) were performed. For electrochemical measurements, 40μl of 1mmoL^{-1} ferriferrocyanide in PBS were used and the experiments were carried out using Iviumstat XR electrochemical analyzer (Eindhoven, The Netherlands). The CV measurements for IEQCM is shown in **Fig. 7(a)**. Based on the oxidation and reduction peaks, a plot of peak current versus scan rate was done as shown in **Fig. 7 (b)**. It can be seen that the anodic and cathodic peak currents were linearly dependent on $\upsilon^{1/2}$ at all scan rates (50-1000 mV/s) for both cases. These results follow the Randles-Sevcik theory which describes that the square root of the scan rate is linear to the peak current. This behavior indicates that the nature of the redox process is diffusion-controlled [33]. From these results, the voltage separation ($\Delta E_p = 150\text{mV}$) was obtained, which agrees typical value in literature which is ~150 mV, indicating that the redox chemistry operates without any major kinetic complications [34].

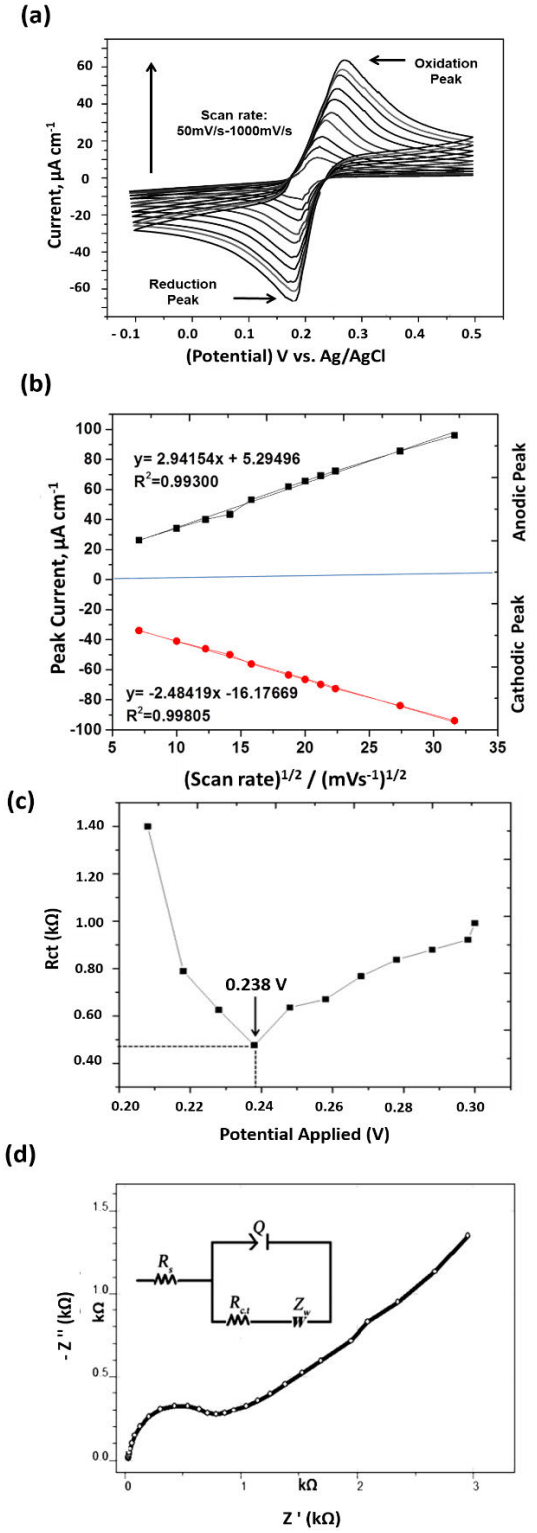

FIGURE 7. (a) Cyclic voltammetry measurements of the IEQCM sensor using ferriferrocyanide in PBS at different scan rates (50-1000 mV/s). (b) Plots of the anodic and cathodic peak currents of Fe $(CN)_6^{3-/4-}$ gold on quartz vs $v^{1/2}$ from cyclic voltammetry measurements. (c) Optimization of applied potential where values of *Rct* was measured at different applied potentials. (c). Nyquist plot at optimized potential, 0.238 V.

Next, the applied potential value was varied from 0.2 V to 0.3 V to obtain the lowest value of R_{ct} and the optimized oxidation peak potential as shown in **Fig. 7(c)**. After that, the Nyquist plot was obtained using the same mediator, $[Fe(CN)_6]^{3-/4}$ with 5 mV amplitude AC input swept at frequencies ranging 1000 kHz to 0.01 Hz and shown in **Fig. 7(d).** The impedance spectra was fitted to the electrical equivalent circuit and the values of solution resistance, $R_S = 30\ \Omega$, charge transfer resistance, $R_{ct} = 476\ \Omega$ and constant phase element, CPE $= 0.1418 \times 10^{-3}$ F. The semi-circular section of the graph indicates small charge transfer resistance, whereas the linear part of the plot showed diffusion control between the mediator and the bare gold electrode. From these results, it was observed that sensing system has both diffusion and charge transfer resistance. These results suggested that the current generation is optimized at lower applied potentials in this work.

TABLE 1. Comparison of EQCM sensors.

Ref	Number of sensors	Discrete Electrode system	Applications	Sample volume
[35]	1	Yes	Fish hormone	5 mL- 6 mL
[36]	2	No	Cells	1.35 mL - 1.5mL
[37]	1	Yes	Biofunctional multilayer films	Not mentioned
[38]	1	Yes	Epinephrine	1mL
[13]	1	No	Explosives	4µL
This Work	12	No		1µL - 10µL

V. CONCLUSION

In this study, twelve integrated electrochemical quartz crystal microbalances were designed and fabricated on a single quartz wafer. EQCM sensors have the advantages of allowing two-dimensional sensing namely: QCM sorption and amperometric electrochemical reactivity. Simultaneous sensing with these two orthogonal methods provides additional selectivity to the sensor and improving detection accuracy. The design parameters such as electrode gap, radius and spacing between sensors were optimized to cater for both sensing methods. To improve electrochemical sensing, the electrode gap was minimized within fabrication limits to increase capacitance and current density of the electrodes. For the quartz crystal microbalance, the electrode radius plays an important role where larger sized electrodes produce resonance frequencies with higher quality factor. The radius of the QCMs are limited by the size of the wafer and the number of sensors to be placed within the same substrate. Spacing between sensors are also crucial to avoid acoustic interference.

The IEQCM sensors were fabricated a combination of evaporated gold and screen-printed Ag/AgCl reference electrodes. The sensors surface roughness and wettability were characterized using AFM and contact angle measurements.

The evaporated gold electrodes produced a hydrophilic surface with low contact angle and low surface roughness compared to commercial screen printed sensors. Experimental measurements of the resonance frequencies show good agreement between the theoretical, simulation and experimental results with errors within 5%. Functionality of the sensors were also tested by placing 1uL – 10 uL liquid water droplets on the sensing electrode and measuring the frequency changes. These frequency changes were translated into mass/area measurements using Sauerbrey equation. The QCM sensor exhibits spatial sensitivity, where the location of the water droplets affects the mass measurements.

Table 1 shows comparison between the fabricated IEQCM with other reported EQCMs. This work shows advantages in terms of it being small, allowing a large number of sensors to be integrated within a single substrate. The large array can be multiplexed to potentiostats and is advantageous when testing several biological samples as well as when performing differential measurements within the same environment. The sensor size ∼10 cm is portable when combined with a portable potentiostat and QCM reader. This IEQCM also requires very low sample volumes of less than 10 uL, compared to discrete EQCMs which require mL samples. Based on the results of this work, it can be seen that multichannel, integrated IEQCM sensor has very good potential as a biosensor for future applications.

ACKNOWLEDGMENT

The collaborative research work was done between Linkoping University, Sweden, XLIM Research Institute, and International Islamic University Malaysia.

REFERENCES

[1] B. Wyszynski and T. Nakamoto, "Linking biological and artificial olfaction: Biomimetic quartz crystal microbalance odor sensors," *IEEJ Trans. Electr. Electron. Eng.*, vol. 4, no. 3, pp. 334–338, May 2009.

[2] K. A. Marx, "Quartz crystal microbalance: A useful tool for studying thin polymer films and complex biomolecular systems at the solution-surface interface," *Biomacromolecules*, vol. 4, no. 5, pp. 1099–1120, Sep. 2003.

[3] Y. Uludağ, S. A. Piletsky, A. P. F. Turner, and M. A. Cooper, "Piezoelectric sensors based on molecular imprinted polymers for detection of low molecular mass analytes," *FEBS J.*, vol. 274, no. 21, pp. 5471–5480, Nov. 2007.

[4] X. Su, F. T. Chew, and S. F. Y. Li, "Design and application of piezoelectric quartz crystal-based immunoassay," *Anal. Sci.*, vol. 16, no. 2, pp. 107–114, 2000.

[5] K. D. Pavey, "Quartz crystal analytical sensors: The future of label-free, real-time diagnostics?" *Expert Rev. Mol. Diag.*, vol. 2, no. 2, pp. 173–186, Mar. 2002.

[6] A. Afzal, A. Mujahid, R. Schirhagl, S. Bajwa, U. Latif, and S. Feroz, "Gravimetric viral diagnostics: QCM based biosensors for early detection of viruses," *Chemosensors*, vol. 5, no. 1, p. 7, Feb. 2017.

[7] L. Du, C. Wu, H. Peng, L. Zou, L. Zhao, L. Huang, and P. Wang, "Piezoelectric olfactory receptor biosensor prepared by aptamer-assisted immobilization," *Sens. Actuators B, Chem.*, vol. 187, pp. 481–487, Oct. 2013.

[8] T. Wasilewski, B. Szulczyński, W. Kamysz, J. Gębicki, and J. Namieśnik, "Evaluation of three peptide immobilization techniques on a QCM surface related to acetaldehyde responses in the gas phase," *Sensors*, vol. 18, no. 11, p. 3942, Nov. 2018.

[9] K. Jaruwongrungsee, U. Waiwijit, A. Wisitsoraat, M. Sangworasil, C. Pintavirooj, and A. Tuantranont, "Real-time multianalyte biosensors based on interference-free multichannel monolithic quartz crystal microbalance," *Biosensors Bioelectron.*, vol. 67, pp. 576–581, May 2015.

[10] F. Shen, K. H. Lee, S. J. O'Shea, P. Lu, and T. Y. Ng, "Frequency interference between two quartz crystal microbalances," *IEEE Sensors J.*, vol. 3, no. 3, pp. 274–281, Jun. 2003.

[11] V. N. Hung, T. Abe, P. N. Minh, and M. Esashi, "Miniaturized, highly sensitive single-chip multichannel quartz-crystal microbalance," *Appl. Phys. Lett.*, vol. 81, no. 26, pp. 5069–5071, Dec. 2002.

[12] F. N. Dultsev, "Quartz crystal microbalance in the active mode as a tool to modify sensor surface for higher selectivity and sensitivity," *Sens. Actuators B, Chem.*, vol. 239, pp. 494–500, Feb. 2017.

[13] L. Yu, Y. Huang, X. Jin, A. J. Mason, and X. Zeng, "Ionic liquid thin layer EQCM explosives sensor," *Sens. Actuators B, Chem.*, vol. 140, no. 2, pp. 363–370, Jul. 2009.

[14] A. A. Zainuddin, A. F. M. Mansor, R. A. Rahim, and A. N. Nordin, "Optimization of printing techniques for electrochemical biosensors," in *Proc. AIP Conf.*, vol. 1808, 2017, Art. no. 020066.

[15] A. A. Zainuddin, "Development of integrated electrochemical-quartz crystal microbalance biosensor arrays: Towards ultrasensitive, multiplexed and rapid point-of-care dengue detection," in *Proc. 12th Int. Conf. Biomed. Electron. Devices, 12th Int. Joint Conf. Biomed. Eng. Syst. Technol. (BIOSTEC BIODEVICES)*, 2019, pp. 220–227.

[16] A. A. Zainuddin, A. N. Nordin, R. A. Rahim, and W. C. Mak, "Modeling of a novel biosensor with integrated mass and electrochemical sensing capabilities," in *Proc. IEEE-EMBS Conf. Biomed. Eng. Sci. (IECBES)*, Dec. 2017, pp. 420–425.

[17] A. A. Zainuddin, A. N. Nordin, R. A. Rahim, A. A. M. Ralib, S. Khan, C. Guines, M. Chatras, and A. Pothier, "Verification of quartz crystal microbalance array using vector network analyzer and OpenQCM," *Indones. J. Electr. Eng. Comput. Sci.*, vol. 10, no. 1, p. 84, Jan. 2019.

[18] J. Hu and X. Huang, "QCM mass sensitivity analysis based on finite element method," *IEEE Trans. Appl. Supercond.*, vol. 29, no. 2, pp. 1–4, Mar. 2019.

[19] X.-H. Huang, W. Pan, J.-G. Hu, and Q.-S. Bai, "The exploration and confirmation of the maximum mass sensitivity of quartz crystal microbalance," *IEEE Trans. Ultrason., Ferroelectr., Freq. Control*, vol. 65, no. 10, pp. 1888–1892, Oct. 2018.

[20] M. Michalzik, R. Wilke, and S. Büttgenbach, "Miniaturized QCM-based flow system for immunosensor application in liquid," *Sens. Actuators B, Chem.*, vols. 111–112, pp. 410–415, Nov. 2005.

[21] J. Rickert, A. Brecht, and W. Göpel, "QCM operation in liquids: Constant sensitivity during formation of extended protein multilayers by affinity," *Anal. Chem.*, vol. 69, no. 7, pp. 1441–1448, Apr. 1997.

[22] J. Kankare, "Sauerbrey equation of quartz crystal microbalance in liquid medium," *Langmuir*, vol. 18, no. 18, pp. 7092–7094, Sep. 2002.

[23] Y.-C. Kuo, C.-S. Chen, K.-N. Chang, C.-T. Lin, and C.-K. Lee, "Sensitivity improvement of a miniaturized label-free electrochemical impedance biosensor by electrode edge effect," *J. Micro/Nanolith. MEMS MOEMS*, vol. 13, no. 3, Sep. 2014, Art. no. 033019.

[24] S. M. Park and J. S. Yoo, "Electrochemical impedance spectroscopy for better electrochemical measurements," *Anal. Chem.*, vol. 75, no. 21, pp.455A–461A, Nov. 2003.

[25] M. Yoda, "Nanogap Biosensors," in *Encyclopedia of Nanotechnology*. Dordrecht, The Netherlands: Springer, 2012, pp. 1544–1552.

[26] A. A. Thyparambil, Y. Wei, and R. A. Latour, "Determination of peptide–surface adsorption free energy for material surfaces not conducive to SPR or QCM using AFM," *Langmuir*, vol. 28, no. 13, pp. 5687–5694, Apr. 2012.

[27] S. Damiati, C. Haslam, S. Sopstad, M. Peacock, T. Whitley, P. Davey, and S. A. Awan, "Sensitivity comparison of macro-and micro-electrochemical biosensors for human chorionic gonadotropin (hCG) biomarker detection," *IEEE Access*, vol. 7, pp. 94048–94058, 2019.

[28] E. Drioli, A. Criscuoli, and E. Curcio, "Membrane materials," *Membr. Sci. Technol.*, vol. 11, pp. 40–104, Jan. 2006.

[29] S. M. Garner, *Flexible Glass: Enabling Thin, Lightweight, and Flexible Electronics*. Hoboken, NJ, USA: Wiley, 2017, pp.168–173.

[30] Z. Hajdari, H. O. Ćurković, V. Čadež, and S. Šegota, "Corrosion protection of cupronickel alloy by self-assembled films of fatty acids," *J. Electrochem. Soc.*, vol. 163, no. 5, pp. C145–C155, 2016.

[31] A. T. Zielinski, A. Prasad, A. A. Seshia, M. Kalberer, and R. L. Jones, "Effects of spatial sensitivity on mass sensing with bulk acoustic mode resonators," *Sens. Actuators A, Phys.*, vol. 236, pp. 369–379, Dec. 2015.

[32] F. Neumann, N. Madaboosi, I. Hernández-Neuta, J. Salas, A. Ahlford, V. Mecea, and M. Nilsson, "QCM mass underestimation in molecular biotechnology: Proximity ligation assay for norovirus detection as a case study," *Sens. Actuators B, Chem.*, vol. 273, pp. 742–750, Nov. 2018.

[33] M. E. Tessensohn and R. D. Webster, "Using voltammetry to measure hydrogen-bonding interactions in non-aqueous solvents: A mini-review," *Electrochem. Commun.*, vol. 62, pp. 38–43, Jan. 2016.
[34] M. Burgess, K. Hernández-Burgos, K. J. Cheng, J. S. Moore, and J. Rodríguez-López, "Impact of electrolyte composition on the reactivity of a redox active polymer studied through surface interrogation and ion-sensitive scanning electrochemical microscopy," *Analyst*, vol. 141, no. 12, pp. 3842–3850, Mar. 2016.
[35] M. Pali, J. E. Garvey, B. Small, and I. I. Suni, "Detection of fish hormones by electrochemical impedance spectroscopy and quartz crystal microbalance," *Sens. Bio-Sensing Res.*, vol. 13, pp. 1–8, Apr. 2017.
[36] M. Oberleitner, "QCM-ECIS: Combined viscoelastic and dielectric sensing of cells," in *Label-Free and Multi-Parametric Monitoring of Cell-Based Assays With Substrate-Embedded Sensors*. Cham, Switzerland: Springer, 2018, pp. 151–293.
[37] J. Li, D. Maniar, X. Qu, H. Liu, C.-Y. Tsao, E. Kim, W. E. Bentley, C. Liu, and G. F. Payne, "Coupling self-assembly mechanisms to fabricate molecularly and electrically responsive films," *Biomacromolecules*, vol. 20, no. 2, pp. 969–978, Feb. 2019.
[38] J. Srivastava, A. Kushwaha, and M. Singh, "Imprinted graphene-starch nanocomposite matrix-anchored EQCM platform for highly selective sensing of epinephrine," *Nano*, vol. 13, no. 11, Nov. 2018, Art. no. 1850131.

AHMAD ANWAR ZAINUDDIN was born in Kuala Lumpur. He received the bachelor's degree in communication engineering and the M.Sc. degree in electronic engineering from International Islamic University Malaysia (IIUM), in 2011 and 2014, respectively, where he is currently pursuing the Ph.D. degree. In 2011, he worked as a Micro-Electro-Mechanical Systems (MEMS) Engineer with Silterra Malaysia. His research interests include medical biosensors, computational mechanics, structural dynamics, smart materials and structures, and modeling of MEMS devices and fundamental of sciences and mathematics.

ANIS NURASHIKIN NORDIN received the B.Eng. degree in computer engineering from International Islamic University Malaysia (IIUM), and the M.Sc. and D.Sc. degrees in microelectronics and VLSI from The George Washington University. She is currently a Professor with the Electronics Engineering Department, IIUM. She has extensive international collaborative networks. She has served as an Invited Researcher for Linkoping University, Sweden, The City College of New York, NY, USA, Griffith University, Australia, and the University of Twente, Holland, The Netherlands. Her work has been published both locally and internationally in more than 100 articles in journals and proceedings. She currently holds two US-patents on MEMS SAW devices. Her research areas are personalized healthcare devices, MEMS, BioMEMS, SAW devices, printed devices, and microfluidics.

AHMAD FAIRUZABADI MOHD MANSOR received the bachelor's and master's degrees from the Department of Electrical and Computer Engineering, International Islamic University Malaysia, in 2013 and 2016, respectively, where he is currently pursuing the Ph.D. degree. His research interests include electric cell-substrate impedance sensing (ECIS) technology, biosensor design, fabrication and application, and biosensing system design.

ROSMINAZUIN AB RAHIM received the B.Eng. degree (Hons.) in electrical and electronics engineering from Universiti Sains Malaysia, in 1999, and the M.Sc. and Ph.D. degrees in microelectronics from Universiti Kebangsaan Malaysia, in 2004 and 2012, respectively. She is currently an Assistant Professor with the Electronics Engineering Department, International Islamic University Malaysia. Her research areas are MEMS, microfabrication technologies, piezoelectric energy harvester, MEMS, BioMEMS, SAW devices, and printed electronics.

WING CHEUNG MAK is currently an Associate Professor (Docent) and the Head of the Biosensors and Bioelectronics Unit with the Department of Physics, Chemistry and Biology, Linköping University, Sweden. He has more than fifteen years' international research experiences in Sweden, Singapore, Germany, and Hong Kong in the field of biosensors and materials sciences. He has authored over 60 peer-reviewed research articles covering the fields in biosensors, bioelectronics, analytical chemistry, materials science and biomedical engineering. His research activities are focus on biosensors and bioelectronics, lateral flow membrane-based biosensors and analytical chemistry, and with strong interest on advanced material design and fabrication strategies to improve biosensor performance.